

# Nebula: Self-Attention for Dynamic Malware Analysis

Dmitrijs Trizna

dtrizna@microsoft.com

Microsoft Corporation, Czech Republic  
University of Genova, Italy

Battista Biggio

battista.biggio@unica.it

University of Cagliari and Pluribus One, Italy

Luca Demetrio

luca.demetrio@unige.it

University of Genova and Pluribus One, Italy

Fabio Roli

fabio.roli@unige.it

University of Genova and Pluribus One, Italy

## Abstract

Dynamic analysis enables detecting Windows malware by executing programs in a controlled environment, and storing their actions in log reports. Previous work has started training machine learning models on such reports to perform either malware detection or malware classification. However, most of the approaches (i) have only considered convolutional and long-short term memory networks, (ii) they have been built focusing only on APIs called at runtime, without considering other relevant though heterogeneous sources of information like network and file operations, and (iii) the code and pretrained models are hardly available, hindering reproducibility of results in this research area. In this work, we overcome these limitations by presenting Nebula, a versatile, self-attention transformer-based neural architecture that can generalize across different behavior representations and formats, combining heterogeneous information from dynamic log reports. We show the efficacy of Nebula on three distinct data collections from different dynamic analysis platforms, comparing its performance with previous state-of-the-art models developed for malware detection and classification tasks. We produce an extensive ablation study that showcases how the components of Nebula influence its predictive performance, while enabling it to outperform some competing approaches at very low false positive rates. We conclude our work by inspecting the behavior of Nebula through the application of explainability methods, which highlight that Nebula correctly focuses more on portions of reports that contain malicious activities. We release our code and models at <https://anonymous.4open.science/r/nebula-3185>.

## 1 Introduction

Dynamic malware analysis is a crucial task not only for detecting, but also for understanding the threats that are wide-spread over the entire Internet. Once samples are collected, analysts execute malware inside isolated environments (sandboxes, virtual machines, or emulation), where they list all the actions performed by the program like network and filesystem

access, registry modifications, API calls, and kernel modifications [1, 2]. These are then gathered in the form of textual summaries and reports that are read by humans, who distill the rationale behind the maliciousness of the analyzed sample. As complicated as it reads, this task is both time and resource consuming, since it involves domain experts in the process, and manual labeling. To speed-up this process, analysts often rely on machine learning techniques, by training models on millions of textual reports and then using them to classify future inputs, thus reducing the amount of human work that is needed to complete this daunting task. Currently, machine learning models for dynamic analysis focus on applying Convolutional Neural Networks (CNNs) and Long Short-term Memory (LSTM) models on reports [3–9], given their impressive results in other Natural Language Understanding (NLU) tasks [10–14]. Local patterns learned by convolutional layers provide qualitative features for further analysis with neural architectures, thus reaching state-of-the-art performance in many information security tasks [4, 5, 15, 16], while LSTM models bypass locality limitation and learn global token relationships [10, 11]. However, these proposed schemes are hindered by three main downsides: (i) convolutions only capture local information, discarding the global correlations contained in reports between actions, while LSTM models struggle in modeling sample behavior based on prolonged token sequences, like a chain of API calls with arguments; (ii) most of the proposed techniques solely rely on homogeneous input data, like API calls [3, 5, 9], rather than leveraging more complete and heterogeneous information representing the behavior of malware samples; and (iii) source code, data, and pre-trained models are typically not available for most of the proposed techniques, hindering reproducibility of results.

To overcome these issues, we present Nebula, a machine learning model based on the transformer architecture [12] trained on reports of different nature. Nebula achieves state-of-the-art performance, overtaking most of the proposed solutions, based on convolutional and LSTM networks, thanks to the introduction of the self-attention mechanism. In particular, Nebula both better detects and classifies input malware within

its correct family, providing higher-quality responses to human analysts. This result is achieved under a strict regime of very low false positive rate, which is a crucial aspects for deployed systems [6, 7, 17]. To the best of our knowledge, we are the first to leverage the transformer architecture to tackle both malware detection and classification from dynamic log reports. To better understand the rationale behind its performances, we conduct an extensive ablation study on the components of Nebula, quantifying the individual contribution of each component to the final score. This analysis is intended to provide a foundational reference for future research in this area, equipping researches with insights into the anticipated outcomes when using analogous components. On top of these results, we empirically highlight how Nebula is focusing on the portions of textual reports that contain malicious activity, by studying the activation of the attention mechanism and applying explainability techniques [18, 19]. To foster reproducible results, we do not only share the code and pre-trained models of Nebula, but we also re-implement, re-train and release methods that were not previously shared with the community [4, 9].<sup>1</sup>

We present our work as follows: we first describe the background concepts needed to understand the technical contributions of Nebula (Section 2), where we also categorize all the previous contributions in the field. We continue by detailing the components of Nebula (Section 3), followed by our extensive experimental analysis (Section 4). We conclude the manuscript with an overview of related techniques (Section 5), and with the main limitations and lines of research that can inspire future work (Section 6).

## 2 Dynamic Windows Malware Analysis

This section provides the background information necessary to understand the technical advancements made by Nebula. We initiate our discussion in Section 2.1, where we briefly delve into the landscape of malware and discuss techniques for detecting compromises through the behavioral analysis of system telemetry. Then, in Section 2.2, we outline the main steps required to implement dynamic malware analysis modeling via machine learning. We conclude this section with a comprehensive survey of published models in Section 2.3.

### 2.1 Logs and Behavioral Reports

The issue of identifying unauthorized system access is paramount within the field of cybersecurity. System compromise can have different manifestations depending on impact, like sensitive data exposure or the misuse of computational resources. Threat actors employ a diverse range of methods, from utilizing built-in tools and protocols aligning with a

“living-off-the-land” approach to leveraging stolen credentials or employing social engineering tactics to achieve their goals through legitimate user accounts. Additionally, adversaries often deploy their own software agents, referred to as malware. According to the 2022 Verizon Data Breach Investigation Report [23], malware was responsible for nearly 40% of breaches, highlighting the importance of its detection in ensuring the digital domain’s security. Moreover, efficient analysis of malware capabilities is crucial for comprehensive threat intelligence. Malware analysis can be segregated into static and dynamic methodologies. The former entails the evaluation of software samples without executing them. For instance, malware samples scripted using technologies such as VBScript are analyzed through deobfuscation and string analysis. Binary samples, like those compiled into EXE or DLL formats, are assessed through disassembly or parsing known structures, such as the import address table of portable executable files.

Dynamic software analysis is a sophisticated process that commences with the “detonation” of a sample in a debugging, sandbox, or emulated environment. This process isolates the application, preventing it from impacting other system parts. However, this may result in inconsistent behavior depending on the detonation environment, subsequently generating *dynamic* features suitable for further examination. Machine learning has become a significant element in malware analysis, with efficient modeling schemes proposed for both static and dynamic data structures derived from malware. Within the scope of this paper, we focus solely on modeling schemes applied to dynamic reports. We argue that the modeling of behavioral reports, which convey machine data with a structure that varies based on the execution environment, yet possesses generally common information, is crucial for capturing a broader, more precise understanding of malware behaviors. This, in turn, can lead to enhanced detection rates, automated reverse engineering capabilities, and improved cybersecurity measures.

### 2.2 Machine Learning Pipeline for Dynamic Analysis

We now describe how machine learning can be applied on top of textual reports by introducing three main steps: (i) *data cleaning* to prepare raw data; (ii) *feature extraction* to create a mathematical representation of reports; and (iii) *modeling* the problem and train the final classifier.

**Data cleaning.** Once the behavioral representation of software is acquired, it is important to perform cleaning and normalizing of the report to make the data manageable for further processing. Filters are used to remove unnecessary data and preserve only a specific set of fields, while normalization techniques are applied to systematize values that are stochastic in nature and do not correlate with application behavior like hash-sums or IP addresses. This allows to introduce do-

<sup>1</sup><https://anonymous.4open.science/r/nebula-3185>

Table 1: Dynamic malware analysis modeling techniques.

	Data Cleaning $\psi(z)$	Feature Extraction $\phi(z')$	Model $f(x)$	Size	Code Released
Neurlux [4]	$\times$	Tokenization	CNN, LSTM, Attention	2.8M	$\checkmark$
Gated CNN [9]	API filter	Feature Hashing	CNN, LSTM	0.4M	$\times^a$
Quo.Vadis [3]	API filter	Tokenization	CNN	1.4M	$\checkmark$
JSONGrinder [20]	$\times$	HMIL [21]	MLP	2.4M	$\checkmark^b$
CruParamer [5, 22]	API filter	API “labeling”	CNN, LSTM	–	$\times$
<b>Nebula (ours)</b>	API, network, file, registry filters and normalization	Tokenization	Transformer (Self-Attention)	5.6M	$\checkmark$

<sup>a</sup>Shared with us privately after request

<sup>b</sup>Non-functional

main knowledge [24] and, as shown in Section 4.3, improves the model’s generalization abilities by reducing variability in values irrelevant to the prediction. We denote this step as  $z' = \psi(z)$ , where  $z$  is the raw data collected from the dynamic analysis environment, and  $z'$  is the cleaned and normalized textual data.

**Feature extraction.** As a next step,  $z'$  undergoes feature extraction denoted  $x = \phi(z')$ . As a final step, it produces a numerical array  $x$ , suitable for analysis by machine learning model. Feature extraction  $\phi$  involves a dichotomy between (a) feature engineering or (b) token encoding. Feature engineering involves the manual or automated selection and transformation of relevant features from the cleaned data  $z'$ , for instance, feature hashing applied to API call names [9, 25] or regular expression-based feature extractors [9]. Token encoding involves a tokenization step, which transforms the textual data  $z'$  into a sequence of tokens and a vocabulary  $V$  of all possible tokens. Tokenization can be based on regular expressions like *WhiteSpace* or *WordPunct* [26] tokenizers, or be influenced by a domain knowledge [27, 28], or involve statistical methods like Byte-Pair Encoding (BPE) [29, 30]. The sequence of tokens is then encoded into a numerical array  $x$  using an encoding function  $f$ , which might be as simple as one-hot encoding, be calculated with term frequency-inverse document frequency (TF-IDF) [31], or use embedding function  $f : V \rightarrow \mathbb{R}^d$ , where  $d$  is the embedding dimension [32].

**Modeling.** The final step is to use the numerical array  $x$  as an input to a machine learning model  $f(x)$ , which produces a prediction  $y$  of a malware label. The modeling function can be as simple as linear models like logistic regression. However, for behavioral reports, the best schemes incorporate representations of sequential information. This can be achieved by convolutions, recurrent neural networks or self-attention with positional encoding.

### 2.3 Dynamic Model Review

The landscape of dynamic malware analysis showcases a competitive interplay between commercial solutions and academic

research. Commercial anti-virus (AV) and Endpoint Detection and Response (EDR) products have integrated behavioral analytics into their detection methodologies, forming part of a multi-objective heuristic that leverages both static and dynamic analysis. Unfortunately, a direct comparison between Nebula and commercial AV or EDR products is not feasible due to the proprietary nature of commercial solutions. The behavioral components of their multi-objective heuristics are closed, which prohibits their disentanglement on the user side for comparison purposes. This lack of transparency means that we cannot gauge how much of the overall performance of these commercial solutions is attributed to their behavioral modeling component specifically.

In academic research, we encounter several groundbreaking methodologies in dynamic malware analysis that pose a formidable challenge to the current state-of-the-art. To offer a consolidated view of these promising approaches, we have curated a selection of these solutions in Table 1, systematizing their respective pipelines according to the steps introduced in Section 2.2. A common theme among contemporary academic contributions is the employment of traditional techniques, such as one-dimensional convolutions, optionally complemented with recurrent layers through Long Short-Term Memory (LSTM) [10], as part of their core modeling approach  $f$ . However, each of these methodologies introduces a unique approach in either data cleaning ( $\psi$ ) or feature extraction ( $\phi$ ) processes, thereby diversifying the analytical landscape of dynamic malware analysis.

**Neurlux (Jindal et al. [4]).** A distinctive feature of this approach is the absence of operations during the data cleaning phase ( $\psi$ ), passing raw behavioral reports directly to the feature extraction process ( $\phi$ ). This phase involves a simple whitespace tokenization procedure and sequences encoding with a vocabulary size of  $V = 10,000$ . The resulting sequences are then modeled  $f$  using a combination of one-dimensional convolutions, Long Short-Term Memory (LSTM), and conventional attention mechanisms [11], which is applied to the output of the LSTM layer. Their code is publicly accessible; therefore, we are able to compare our

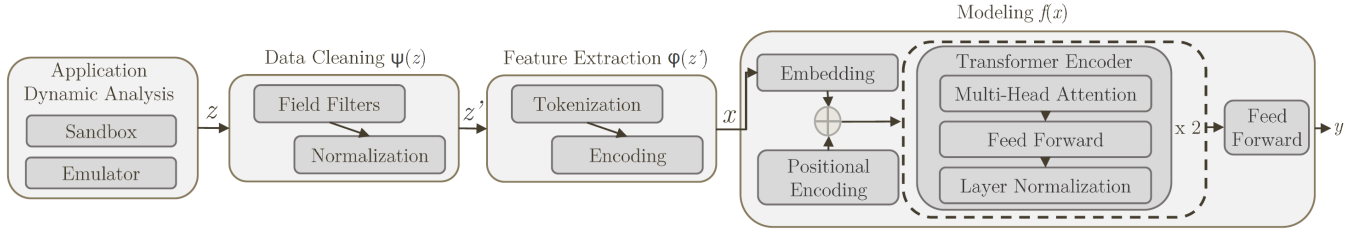


Figure 1: A schematic overview of Nebula.

results with this model. However, the data utilized in their research remains undisclosed.

**Gated CNN (Zhang et al. [9]).** This model introduced an analysis where  $\psi$  preserves only API call data, each undergoing a custom feature engineering process during  $\phi$  phase. Then, the sequence of featurized vectors is modeled through a gated convolution network as  $f$ . While the code for their model is not released publicly, it was provided by the researchers upon request, enabling us to draw a direct comparison between our results and their model. However, similar to the case of Neurlux, the data utilized in their study has not been released.

**Quo.Vadis (Trizna [3]).** This hybrid model simultaneously assesses contextual, static, and dynamic features. Their model code is released publicly, which significantly contributes to the transparency of their work. For our analysis, we concentrated on the dynamic component of their pipeline, which data cleaning  $\psi$  preserves only API call names. Feature extraction  $\phi$  label-encodes each API call name with a vocabulary of  $V = 600$  and subsequently models  $f$  with a 1d convolutional neural network. This work is especially notable for its public release of a comprehensive dataset consisting of Speakeasy [33] emulation reports. This allows for the pursuance of both malware detection and type classification objectives.

**JSONGrinder (Bosansky et al. [20]).** This model provides a unique method for parsing hierarchical JSON reports, originally proposed in [21]. This method employs a combination of Julia libraries, specifically `JsonGrinder.jl` used for feature extraction  $\phi$  and `Mill.jl` for modeling  $f$ , data cleaning  $\psi$  is omitted. The  $\phi$  phase infers a Hierarchical Multiple Instance Learning (HMIL) schema from the data, constructing a fixed-size vector, while the modeling is based on a multilayer perceptron (MLP) for sample classification. However, it is worth noting that their implementation was not compatible with the latest version of Julia (v1.8.5) at the time of our experiments, causing the original model implementation to fail without modifications. Additionally, Bosansky et al.’s work is notable for its release of a comprehensive dataset useful for malware family classification, which adds considerable value to the existing body of resources in this field.

**CurParamer (Chen et al. [5, 22]).** This method preserves only API calls from the original report during the data clean-

ing phase ( $\phi$ ). The feature extraction step ( $\psi$ ) involves a unique approach to API labeling and embedding, which includes parameter-assisted API labeling and sensitivity-inspired API embedding. These techniques utilize domain knowledge to generate more efficient numerical representations of API calls. To model these representations ( $f$ ), they employ two separate networks based on 2D convolutions and LSTM. Although their feature extraction methodology is intriguing, it is presented with little implementation details, which reduces its replicability. Despite efforts to access the modeling code, the authors made no public version available, even upon private request.

### 3 Nebula: Transformer Architecture for Dynamic Malware Detection

The design of our dynamic malware analysis pipeline draws from the proven success of the attention mechanism in Natural Language Understanding (NLU). Particularly, the self-attention-based Transformer architecture [12] has demonstrated superior performance over conventional RNN- or CNN-based modeling methods [13, 14, 34]. These successes guided the selection of techniques used during our feature extraction ( $\phi$ ) and modeling ( $f$ ) stages. The most significant deviation from standard NLU pipelines is evident during the data cleaning phase ( $\psi$ ). Here, we employ a domain-specific parser that (i) retains only those fields from the original structured report relevant for behavior generalization; and (ii) normalizes unconstrained and arbitrary values within such selected fields. In the feature extraction phase ( $\phi$ ), we tokenize each report into a sequence of tokens of length  $N$  and encode each token based on a vocabulary of size  $V$ . When modeling this sequence, we first embed the input vector to a higher dimension, apply position encoding, and then process it through a Transformer encoder layer to apply the self-attention operation. The resulting attended tensors are then forwarded to a classifier that produces the final prediction. A high-level overview of our Nebula modeling scheme is depicted in Figure 1.

#### 3.1 Data Cleaning

We detail the data cleaning  $z' = \psi(z)$  applied by Nebula.

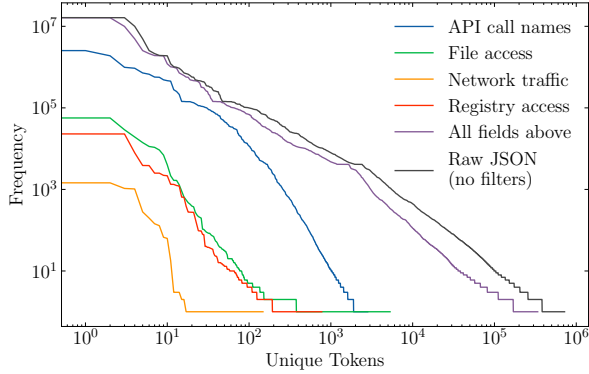


Figure 2: Visualization of whitespace token frequency in the Speakeasy [33] emulated behavioral report training set [3].

**Vocabulary and field filters.** Machine data is more volumetric and heterogeneous than natural languages. Therefore, it can have a significantly larger vocabulary, as no distinct lexical boundaries or grammatical rules define the language being used. In system logs, it is common to see arbitrary character combinations like `/tmp/83afba/setup.bin` or `jre1.8.0_311`, which explode vocabulary given improper handling. For instance, even after path normalization, we observe more than 6000 unique filepaths, where only roughly 400 paths repeat, and the rest appear only once. The Figure 2 visualizes the frequency distribution of tokens for different JSON fields in the Speakeasy emulated behavioral report training set [3]. Every additional field included in the analysis increases the vocabulary size. For instance, given filter that uses API calls, file, network, and registry records total vocabulary size is about 2.5M tokens. Given no filters applied, this number jumps close to 8M tokens, exploding vocabulary more than three times and significantly reducing the epistemic density (valuable information per token) of the data.

Concerning field filtering, existing dynamic malware modeling techniques fall into two categories: do not implement any filters [4], or use only a single type of information, usually API calls [3, 5]. Focus solely on API calls eliminates valuable behavior representations necessary for establishing effective decision boundaries in malware detection. Research has demonstrated that domain experts rely on a broader range of information when performing actual malware analysis [24,35]. Based on ablation studies discussed in Section 4.3, we preserve the following fields from dynamic analysis report: (i) API call names, arguments, and return codes; (ii) file operation type and path; (iii) network connection port and server name; and (iv) registry access type and key value. We found this combination of fields produces the best generalization and the least overfitting. The application of field filters on Speakeasy behavioral report is exemplified in Figure 3. In this redacted illustration, only fields that contain API call and network event information are retained, while irrelevant parts such as `start_addr` or `apihash` are discarded.



Figure 3: Example of unfiltered (left) and filtered (right) Speakeasy [33] behavior reports, illustrating the application of field filters. API call names with arguments and network connection details are retained. Both reports have been redacted for brevity.

**Normalization.** Retained fields still have unbounded or unpredictable values, which may not inherently contribute to the effectiveness of machine learning models. For instance, the exact values of IP addresses are not representative *per se* and primarily provide broader context, such as indicating whether the IP is from a private or public network or what autonomous system it belongs to. Similarly, file paths may contain elements like usernames, drive letters, or randomized file and directory names, which have relative contextual significance for behavioral analysis. Hence, the raw values of such fields may not be directly beneficial for modeling, emphasizing the need for suitable normalization before analysis. We incorporate domain knowledge via placeholders by normalizing filepaths, network connection, and registry access information in the following manner: (i) hash-sums in any field, including SHA1, SHA256, and MD5, are substituted with placeholders like `<sha1>`, `<sha256>`, `<md5>` placeholders; (ii) IP addresses are mapped to placeholders symbolizing loopback, private, public, or IPv6 addresses; (iii) recognizable domain names associated with a list of common top-level domains such as `com` or `net` (but not exclusive to these) are assigned the `<domain>` placeholder; (iv) Windows path variables, for instance, `%windir%` or `%userprofile%`, are expanded to a full path; and (v) frequent Windows paths patterns are replaced with specific placeholders such as `<drive>` or `<user>`.

### 3.2 Feature Extraction

We now detail the feature extraction  $x = \phi(z')$  applied after the data cleaning phase  $\psi$  by Nebula.

**Tokenization.** The next phase in dynamic report processing involves breaking down the normalized text sequence into individual tokens suitable for encoding. We decided to test several prevalent modes of tokenization – Byte Pair Encoding (BPE) [29], Whitespace, and Wordpuct. Whitespace tokenization is a straightforward scheme that uses regular expressions to split the text. It creates tokens by separating words based on spaces, tabs, and newline characters. In essence, this method views each word or punctuation as a standalone token. Wordpunct uses similar regular expression-based logic that, in addition to whitespace symbols, uses punctuation to split tokens. We implement both tokenizers mentioned above using NLTK library [26]. An fragment of whitespace tokenized dynamic analysis report:

```
"0x0", "0x1", "kernel32.getProcAddress",
"0x1000", "0xfa", "kernel32.tlsgetvalue"
```

BPE is a more sophisticated approach. It tokenizes text based on frequently occurring byte pairs within the data. Initially, each character in the text is considered a token. The algorithm then iteratively merges the most common pair of consecutive tokens to form new tokens, repeating this process until a specified number of merges have been completed, or no further merges can be made. We utilize the SentencePiece [30] library to implement BPE. The redacted set of BPE tokens covering the same dynamic analysis report fragment are as follows:

```
"0x", "0x1", "ne", "32.", "kernel32.", "et",
"ad", "getproc", "10", "0xf", "tls", "val"
```

Furthermore, for both tokenization schemes, we limit our vocabulary to  $V = 50000$  most common tokens and introduce two special tokens to denote all other tokens (<unk>) and padding of shorter sequences (<pad>).

**Sequence length.** In the case of machine data, the tokenized sequences from system log events are typically lengthy. To manage this, we confine behavioral reports to the first  $N$  tokens. By keeping the computational budget constant, we evaluate the performance of models with varying sequence lengths. The results of these comparative studies, often referred to as ablation studies, will be detailed in Section 4.3, with the final choice of  $N = 512$ .

### 3.3 Model Architecture

We now detail the last component of Nebula, which is the model function  $f$ .

**Embedding and positional encoding.** Embedding operation maps the input sequence of integers to a higher dimensional space:  $e = E(x) \cdot \sqrt{d_e}$ , where  $E(x)$  is the embedding of the input  $x$  and  $d_e$  is the dimension of the embedding,

with square root used for scaling. This results in vector  $e = [e_1, e_2, \dots, e_{pos}, \dots, e_N]$ , where  $e_{pos} \in \mathbb{R}^{d_e}$ .

Since our method relies on the Transformer architecture [12], which lacks the inherent sense of order provided by recurrent models, we need to incorporate positional information in our sequence. There are multiple alternative ways to encode position [36]. We replicate the approach introduced by Vaswani et al. [12], creating a set of sinusoidal functions with different frequencies for each position in the sequence:

$$PE_{(pos, 2i)} = \sin\left(\frac{pos}{10000^{2i/d}}\right), \quad (1)$$

$$PE_{(pos, 2i+1)} = \cos\left(\frac{pos}{10000^{2i/d}}\right), \quad (2)$$

where  $PE_{(pos, i)}$  is the  $i$ -th dimension of the positional encoding of the token at position  $pos$  in the sequence, and  $d$  is the dimensionality of the model. The  $PE_{(pos, 2i)}$  and  $PE_{(pos, 2i+1)}$  terms are used for even and odd dimension  $i$  respectively. These values are then added to the embedded vectors  $e_{pos}$  to incorporate the positional information into the sequence  $e'_{pos} = e_{pos} + PE_{pos}$  where  $PE_{pos} = [PE_{(pos, 1)}, PE_{(pos, 2)}, \dots, PE_{(pos, d)}]$  is the positional encoding vector for position  $pos$ . The result is a sequence of vectors  $e' = [e'_1, e'_2, \dots, e'_N]$ , where each vector represents both the token semantics and its position in the sequence, which can now be fed into the Transformer network.

**Neural layers.** Our architecture leverages Transformer architecture, which originally employs both encoder and decoder layers [12]. Our setup utilizes only encoder layers similar to Devlin et al. [14], a design choice that aligns our model with inference task rather than generative objectives as in applications that include decoder [12, 13]. We employ two Transformer encoder layers that align our model size with those of comparable models in Table 1. This choice is not restrictive – the model can be scaled up to incorporate more Transformer layers to improve performance, consistent with the principle of model scaling laws [37]. After the self-attention operation, data is forwarded to a classifier for the final prediction. In our implementation, the classifier consists of a fully connected neural network with a single hidden layer composed of 64 neurons and the final layer for binary or multi-class classification.

**Reduced self-attention span.** Input comprised from structured machine data like malware behavior reports contain information in lengthy sequences, which poses a challenge for self-attention architectures like Transformer [12] since such models exhibit quadratic complexity with respect to the sequence length. The self-attention operation can be represented as:

$$\text{Attention}(Q, K, V) = \text{softmax}\left(\frac{QK^T}{\sqrt{d_k}}\right)V, \quad (3)$$

Table 2: Number of samples per malware family in Avast-CTU Dataset [20].

Family	Adload	Emotet	HarHar	Lokibot	njRAT	Qakbot	Swisyn	Trickbot	Ursnif	Zeus	Total
Samples	704	14429	655	4191	3372	4895	12591	4202	1343	2594	54000

where  $Q$ ,  $K$ , and  $V$  as queries, keys, and values, respectively used as inputs to a self-attention layer, and  $d_k$  is the dimension of the keys. The product  $QK^T$  results in a matrix of size  $N \times N$ , where  $N$  is the sequence length. Calculating this product has a complexity of  $O(N^2)$ , leading to the quadratic computational complexity with respect to the sequence length.

We propose an alternative approach to reduce computational complexity by partitioning the self-attention operation described in Equation 3 into several independent attention spans instead of applying it to the entire sequence. Assume that the original sequence length  $N$  is divisible by the span  $S$ , so there are  $M = N/S$  spans. Let  $Q_i$ ,  $K_i$ , and  $V_i$  denote the queries, keys, and values for the  $i^{th}$  span. Then,  $\text{Attention}(Q_i, K_i, V_i) \quad \forall i \in \{1, 2, \dots, M\}$  and independent attention results are concatenated to an original size vector  $N$ .

In this way, the complexity is reduced to  $O(MS^2)$ , improving the model’s computational efficiency, especially when  $S \ll N$ . Our experiments use  $S = 64$  with  $N = 512$ , resulting in  $M = 8$  independent self-attention spans. We observe that reducing attention spans enhances the model’s inferential capacity on behavioral reports while adhering to the same computational constraints.

## 4 Experimental Evaluation

The following section presents an in-depth experimental evaluation designed to assess the effectiveness and robustness of Nebula. In Section 4.1, we discuss the datasets used for our experiments. We outline our experimental setup in Section 4.2, including details about the model training and evaluation metrics, and providing a comprehensive view of our methodology. Section 4.3 dives into ablation studies, which assess the impact of each component of Nebula on the overall model’s performance. In Section 4.4, we compare Nebula with other dynamic analysis models expressing state-of-the-art potential. This comparative analysis gives us a clearer understanding of where Nebula stands in relation to other techniques in the field, highlighting its strengths and areas for improvement. Finally, Section 4.5 focuses on the explainability of Nebula’s heuristic. As machine learning models become increasingly complex, interpretability is paramount for trust and practical applicability.

### 4.1 Datasets

In our experiments, we evaluate three publicly available datasets that contain dynamic malware analysis reports by

Table 3: Speakeasy Dataset [3] structure and size.

Sample label	Training set		Test set	
	Size (Gb)	Count	Size (Gb)	Count
<i>Benignware</i>	127.0	26061	47.0	10000
Backdoor	30.0	11089	7.4	2500
Coinminer	46.0	10044	11.0	2500
Dropper	36.0	11275	9.0	2500
Keylogger	34.0	7817	9.8	2500
Ransomw.	14.0	10014	4.6	2500
RAT	5.5	9537	2.5	2500
Trojan	40.0	13128	7.1	2500
<b>Total</b>	329	98966	98	27500

discussing two different types of analysis.

**Malware detection.** This binary classification task discerns between benign and malicious software. It’s a fundamental task performed by AV and EDR solutions with the aim of detecting malevolent logic running on a system. In real-world applications, it is paramount to maintain severely low false-positive rates to ensure usability and efficiency.

**Malware classification.** This is a multi-label classification objective, targeting the attribution of malware samples to a specific type or family. Threat intelligence teams often execute it to study the evolution of malware strains, uncover shared characteristics, and identify potential countermeasures.

We now characterize each dataset by its sample size, the environment used for data collection, its applicability for either malware detection and classification tasks, and the availability of separate training and test sets.

**Speakeasy Dataset [3].** This dataset<sup>2</sup> was generated using Speakeasy v1.5.9 [33], a Windows kernel emulator, comprising behavioral reports from in total approximately 93,500 samples, with both legitimate and malicious reports formatted in JSON. The malicious samples belong to seven distinct malware types, with sample prevalence across labels detailed in Table 3. Therefore, the dataset is suitable for both malware detection and classification tasks. The dataset provides a test set explicitly, collected in a different timeframe (April 2022) from the training set (January 2022). This temporal separation facilitates the examination of concept drift in malware behavior.

**Avast-CTU Dataset [20].** This dataset<sup>3</sup> houses sandbox re-

<sup>2</sup><https://www.kaggle.com/ds/3231810>

<sup>3</sup><https://github.com/avast/avast-ctu-cape-dataset>

ports in JSON format derived from CAPEv2 [38] (a Cuckoo sandbox [39] derivative), with approximately 400,000 samples collected between January 2017 and January 2020. The reports represent ten different malware families (Table 2). Due to the absence of legitimate samples, this dataset is solely used for malware classification tasks. The dataset formation aligns with the splitting approach recommended by Bosnansky et al. [20], in which all samples preceding August 2019 are designated as the training set, while the remainder forms the test set.

**Malicious Code Dataset (MCD) [40].** This dataset has approximately 30,000 labeled samples containing API call sequences in XML format without any additional behavioral data (such as filesystem, registry, or network access). The dataset’s collection methodology and the environment are not explicitly detailed. The training set contains 10,000 malware and 20,000 goodware samples. As no malware family or type labels are available, this dataset is solely applicable for malware detection task. The test set with 15,000 unlabeled samples cannot be used for evaluation due to the lack of labels. Hence we report mean metrics only on validation sets through cross-validation folds.

## 4.2 Experimental Setup

Our experiments were conducted on an NVIDIA Quadro T2000, a standard consumer GPU. To align with the limitations of the hardware capacity, the batch size was fixed at  $b = 96$  for all experiments. For optimization, we employed the AdamW optimizer [41] with a static learning rate of  $\alpha = 2.5^{-4}$ . The hyperparameters were set as  $\beta_1 = 0.9$ ,  $\beta_2 = 0.999$ , and  $\epsilon = 10^{-8}$ . An  $L_2$  regularization with a weight decay of  $\lambda = 1e^{-2}$  was also implemented. The evaluation metrics were derived from three cross-validation (CV) folds on the training set. The reported metrics are the mean values of the three models evaluated on the validation subsets and a single test set.

To ensure fair evaluation given the variations in model size as indicated in Table 1, we maintained a constant time budget for training instead of a fixed number of epochs. Each fold was allocated a training duration of five minutes, resulting in a total training budget of 15 minutes per cross-validation run for three folds, excluding pre-processing time. Initial experiments with longer training runs, such as an hour per cross-validation, yielded similar relative outcomes with tolerable deviations. As such, the 15-minute training budget was deemed optimal for subsequent experiments.

## 4.3 Ablation Studies

In this section, we explore the impact of variations in model components and their configurations on the final performance of the Transformer model. This serves to highlight the effectiveness of individual components in the context of the

Table 4: Mean validation set metrics over three CV folds with different vocabulary sizes on Speakeasy data. Reported TPR is at  $FPR = 10^{-3}$ .

Metric	5k	10k	30k	50K	70k
TPR	0.8078	0.7834	<b>0.8576</b>	0.8383	0.8407
AUC	0.9965	0.9969	<b>0.9977</b>	0.9976	<b>0.9977</b>
F1	0.9817	0.9839	0.9861	0.9856	<b>0.9862</b>
Acc.	0.9753	0.9782	0.9811	0.9806	<b>0.9814</b>

model’s overall performance. For our ablation experiments, we utilize Speakeasy Dataset as it offers a comprehensive range of behavioral representations. Furthermore, this data enables us to evaluate malware detection performance using a binary classification objective, thereby yielding more interpretable results.

**Vocabulary size.** The impact of varying vocabulary size on the performance of the model using the Speakeasy emulation data is presented in Table 4. The results demonstrate marginal differences in performance within the range of vocabulary size  $V \in \{30\,000, \dots, 70\,000\}$ , suggesting that performance in this interval is largely subject to the randomness introduced during model initialization and training. This trend suggests that the model’s performance is relatively stable with respect to variations in vocabulary size within this range, indicating a degree of robustness to this parameter. Considering these observations, we chose  $V = 50\,000$  as a good compromise that balances performance and complexity.

**Field filters.** Initially, we examine the utility of individual fields for malware detection. Figure 4a presents the outcomes of experiments in which only a specific single field from the behavioral report is retained. Notably, the most influential component of behavioral representation is the sequence of API calls, especially when arguments are provided alongside the API names. All other fields exhibit inferior performance when considered in isolation. This observation can be rationalized by recognizing that not every type of malware or emulation generates traces in the filesystem, registry, or network – only a limited subset of emulation reports contain this data. However, all samples invariably exhibit a sequence of API calls, which underscores the critical role of API call information in malware detection. However, the inclusion of filesystem, registry, or network information in conjunction with API calls enhances detection capabilities. This synergy enables the model to capture a more comprehensive representation of the software’s behavior, improving the accuracy and reliability of its predictions.

Additionally, we investigated two preprocessing modalities: (i) a version that abstains from the application of filters, and (ii) one that incorporates optimal field filters during preprocessing. Table 5 presents the F1 scores on the validation and test sets of the Speakeasy emulation reports for both the BPE

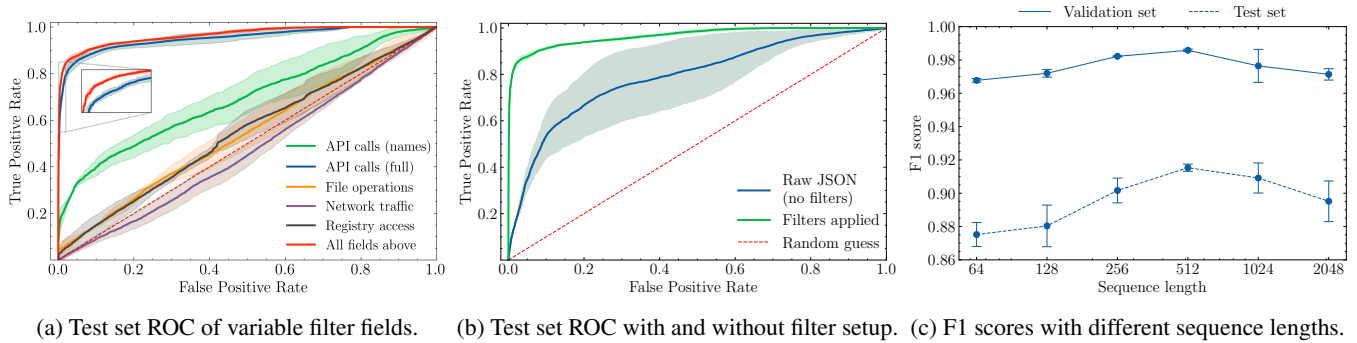


Figure 4: Results of ablation studies under different configurations on Speakeasy dataset.

Table 5: Mean F1 values of field filter ablation studies over three CV folds on Speakeasy dataset.

Fields	Val. set F1	Test set F1	$\Delta$
Raw JSON (BPE)	0.9884	0.7495	<b>0.2389</b>
Raw JSON (whosp.)	0.9899	0.7275	<b>0.2624</b>
Filtered JSON (BPE)	0.9847	0.9136	<i>0.0711</i>
Filt. JSON (whosp.)	0.9870	0.9068	<i>0.0802</i>

and whitespace tokenization schemes. Remarkably, a significant overfitting issue is present when filters are not employed, evidenced by a difference ( $\Delta$ ) in performance between the validation and test sets. While modeling that employs filters lose about 7% – 8% of F1 on the test set, the performance of modeling without filters degrades down by 23% – 25%. A visual examination of this trend is depicted in Figure 4b, where the Receiver Operating Characteristic (ROC) curve for the test set demonstrates significant degradation when filters are not employed. Additionally, the high standard deviation between cross-validation runs suggests a level of model instability or variance in prediction. The observed outcome can be attributed to the presence of unconstrained variables representative of one specific execution, like hash sum or start address memory segment. These fields cause the model to overfit the training data, hindering its generalization and predictive capabilities to unseen data in the test set. Hence, the application of field filters appears instrumental in enhancing model stability and performance, contributing to more reliable and generalizable predictions.

**Tokenization.** We conducted ablation studies on tokenization to investigate the impact of different tokenization strategies on model performance. Three different tokenizers were tested: BPE [30], Whitespace, and Wordpunct [26]. The test set F1 scores for different tokenization methods are reported in Table 6. The results reveal that all three tokenization methods deliver comparable mean F1 scores. The BPE tokenizer demonstrates slightly better generalization capabilities, achieving an F1 score on the test set that is almost 1% higher

Table 6: Mean test set metrics over three CV folds of tokenizer ablation studies on Speakeasy data. TPR is at  $FPR = 10^{-3}$ .

Tokenizer	TPR	AUC	F1	Acc.
Validation set				
Wordpunct	0.8919	<b>0.9979</b>	<b>0.9872</b>	<b>0.9828</b>
Whitespace	<b>0.8965</b>	<b>0.9979</b>	0.9870	0.9824
BPE [29]	0.8208	0.9973	0.9847	0.9793
Test set				
Wordpunct	0.5540	0.9630	0.9049	0.9041
Whitespace	<b>0.5703</b>	<b>0.9664</b>	0.9068	0.9053
BPE	0.5213	0.9657	<b>0.9136</b>	<b>0.9104</b>

than the others. This observation is further supported by the field filter experiments discussed in the previous paragraph, with results in Table 5, where BPE exhibited the smallest performance decrease ( $\Delta$ ) between the validation and test sets. Furthermore, it is noteworthy that the Whitespace tokenizer achieves impressive results on the test set, surpassing the other tokenization methods if evaluated by area under the curve (AUC) or true positive rate (TPR) at false positive rate (FPR) of  $10^{-3}$ , as shown in Table 6. Given competitive performance of BPE and Whitespace, we report metrics of both tokenizers for subsequent malware detection and classification, as well as explainability experiments.

**Sequence length.** Figure 4c depicts the F1 scores on the validation and test sets with varying sequence lengths. It is evident that the performance on both validation and test sets peaks at a sequence length of  $N = 512$ . This suggests that sequences of length  $N \in \{64, \dots, 256\}$  may not encapsulate all the necessary information for effective model inference, leading to a significant drop in test set performance. On the other hand, longer sequences are more computationally demanding, especially when utilizing self-attention-based modeling. Hence, under the same computational time constraints, sequences with length  $N \in [1024, 2048]$  yield less robust results.

Table 7: Malware detection mean metrics over three CV folds on Speakeasy dataset. Reported TPR is at FPR=  $10^{-3}$ .

Model	Training batches	Validation set				Test set			
		TPR	AUC	F1	Acc.	TPR	AUC	F1	Acc.
Gated CNN [9]	1058	0.476	0.9827	0.9411	0.9233	0.2152	0.8879	0.6465	0.7014
Neurlux [4]	7406	0.836	0.9976	0.9847	0.9794	0.4250	0.9528	0.8792	0.8786
Quo.Vadis [3]	4761	0.769	0.9954	0.971	0.9614	0.3081	0.9224	0.8065	0.8173
Nebula (BPE)	<b>2116</b>	0.8208	0.9973	0.9847	0.9793	0.5213	0.9657	<b>0.9136</b>	<b>0.9104</b>
Nebula (whitespace)	2159	<b>0.8965</b>	<b>0.9979</b>	<b>0.9870</b>	<b>0.9824</b>	<b>0.5703</b>	<b>0.9664</b>	0.9058	0.9053

Table 8: Malware detection mean metrics over five CV folds on MCD data. Reported TPR is at FPR=  $10^{-3}$ .

Model	TPR	AUC	F1	Acc.
Neurlux [4]	0.8508	0.9942	<b>0.9687</b>	<b>0.9794</b>
Quo.Vadis [3]	<b>0.9035</b>	<b>0.9950</b>	0.9613	0.9736
Nebula (BPE)	0.8332	0.9937	0.9653	0.9770
Nebula (whitespace)	0.8243	0.9932	0.9590	0.9731

#### 4.4 Comparison with State of the Art

**Malware detection.** In this section, we evaluate the performance of our proposed method, Nebula, with several state-of-the-art models in the domain of malware detection. For all conducted experiments, we report AUC, F1, Accuracy, and True Positive Rate (TPR) at a fixed False Positive Rate (FPR) of  $10^{-3}$ .

Malware detection metrics on the Speakeasy dataset [3] are reported in Table 7 with ROC curve on the test set exemplified in Figure 5. Four modeling techniques with source code available as presented in Table 1 were able to model this data, namely Neurlux presented by Jindal et al. [4], Gated CNN model by Zhang et al. [9], Quo.Vadis released by Trizna [3], and Nebula.

Our model surpasses all competitive architectures on Speakeasy emulation data, outperforming all metrics on validation and test sets in either the whitespace and BPE tokenization modes. This is particularly evident under low false-positive conditions. For instance, with an FPR of  $10^{-3}$ , Nebula with whitespace tokenization demonstrates a detection rate of 0.897 on the validation set and 0.570 on the test set. In comparison, the next best performing model, Neurlux, scores 0.836 and 0.425 on the validation and test sets, respectively. This observation becomes critically significant considering that strict low false positive rates are enforced on production-grade malware detectors [6, 7].

The efficiency of Nebula is also reflected in the number of training batches required. As seen in Table 7, Nebula achieves these results with less than a third of the training batches required by the second-best model, Neurlux. Turning

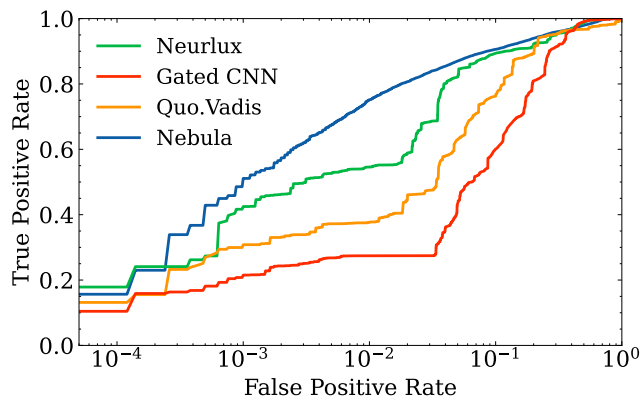


Figure 5: Mean ROC curves over three cross-validations for malware detection of Neurlux [4], Gated CNN [9], Quo.Vadis [3] and Nebula (with BPE tokenizer) on Speakeasy data test set.

awareness to the Malware Code Dataset (MCD) [40], the mean validation set metrics are presented in Table 8. MCD preprocessing is computationally demanding due to the high information density per sample because of lengthy API call traces. This has a detrimental effect on models that employ custom feature engineering schemes, such as Zhang et al. [9], which take several seconds of feature engineering per MCD sample. Processing a training set of 30,000 samples in this manner would take approximately 100 hours—impractical in both experimental and real-world scenarios. Consequently, we excluded this model from our experiments on MCD.

Our observations reveal that Quo.Vadis, a simplistic modeling scheme focused solely on API call names, outperforms both Neurlux and Nebula based on AUC and detection rate under low false-positive conditions. Given the lengthier API call sequences in the MCD data, narrowly focused models like Quo.Vadis might capture more behavior relevant to the data. This outlines the evidence that narrow modeling schemes are still more tuned to this specific data type for specific data sources and can outcompete more general mechanisms.

**Malware classification.** Predicting malware family is a multi-label objective, and we report the results of the performances of the considered models in Table 9 and Table 10 the F1 scores

Table 9: Mean F1 scores over three CV folds for malware classification objective on Speakeasy dataset.

	Clean	Backdoor	Coinminer	Dropper	Keylogger	Ransomware	RAT	Trojan
Neurlux	0.8453	0.8329	<b>0.6910</b>	0.4488	0.2032	0.5527	<b>0.6625</b>	0.6153
Gated CNN	0.7588	0.6870	0.5586	0.2015	0.0794	0.3584	0.0000	0.5282
Quo.Vadis	0.8338	0.8520	0.4884	0.3580	<b>0.2119</b>	0.6861	0.1195	0.5359
Nebula (BPE)	<b>0.8526</b>	<b>0.8548</b>	0.6303	0.2850	0.1295	<b>0.7421</b>	0.3683	<b>0.6827</b>
Nebula (whitsp.)	0.8240	0.8324	0.6214	<b>0.4615</b>	0.1179	0.6523	0.1854	0.6486

Table 10: Mean F1 scores over three CV folds for malware classification objective on Avast-CTU dataset.

	Adload	Emotet	HarHar	Lokibot	Qakbot	Swisyn	Trickbot	Ursnif	Zeus	njRAT
Neurlux	<b>0.7150</b>	0.9294	<b>0.9031</b>	0.8320	0.9320	<b>0.9991</b>	<b>0.9536</b>	0.8910	0.6503	0.8479
Nebula (BPE)	0.4390	<b>0.9392</b>	0.7763	0.8957	<b>0.9876</b>	0.9973	0.9227	0.9362	0.6419	0.8656
Nebula (whitsp.)	0.6975	0.9319	0.8363	<b>0.9048</b>	0.9768	0.9984	0.9056	<b>0.9585</b>	<b>0.6690</b>	<b>0.8896</b>

on the Speakeasy and Avast-CTU datasets. We also report a comprehensive evaluation with other relevant metrics as well for all malware families in [Appendix A](#). Specifically, results on the Speakeasy data can be found in [Table 11](#), while metrics on the Avast-CTU data are detailed in [Table 12](#).

Notable, the Avast-CTU dataset, introduced by Bosansky et al. [20], is characterized by the absence of sequential information. Instead, it provides a summary of behavioral operations conducted within the sandbox by each sample. Consequently, this dataset is *unsuitable* for models that examine sequential patterns in API calls, such as the Quo.Vadis and the Gated CNN. More generalized architectures like Neurlux and Nebula are capable of effectively modeling this data. Thus Avast-CTU analysis includes these models only. Nebula exhibits superior test set F1 scores for 4 out of 7 malware types on Speakeasy ([Table 9](#)) data and in 6 out of 10 malware families on Avast-CTU data ([Table 10](#)). Nebula superiority is particularly noticeable in malware families experiencing significant concept drift, such as polymorphic Emotet [42], in families with many sub-variants, like Zeus [43], or on malware types that exhibit rich and diverse behaviors, such as benignware, backdoors, ransomware, or trojans. *Modus operandi* of such agents require frequent manipulation with network, filesystem, and registry. An examination of metrics on Speakeasy Dataset test set shows that Neurlux still surpasses Nebula in detecting Droppers and RATs, achieving 18% and 30% higher F1 scores, respectively. This might suggest a weakness in Nebula’s data-cleaning approach for these particular malware families, indicating a potential avenue for future improvements. Simultaneously, we note that models focusing solely on API calls, such as Quo.Vadis, exhibit slightly superior performance over the general models for malware families with less diverse behavior on Speakeasy Data. For instance, Quo.Vadis performs better in detecting Keyloggers, a malware type that only occasionally interacts with the network or

filesystem to store logged keys.

## 4.5 Explaining the Behavior of Nebula

We now analyze the behavior of Nebula, by leveraging well-known techniques from the *explainable AI* (XAI) research domain. The first technique, named *Integrated Gradients* [18] computes the importance of input features by integrating gradients along a path from a baseline to the input. In our case, we use an empty JSON file as the baseline, that stands for the absence of any behavior. We leverage the GradientSHAP implementation from the SHapley Additive exPlanations (SHAP) framework [44]. Since this technique requires an end-to-end differentiable model, it is not directly applicable in our case due to the presence of the initial embedding layer. To overcome this issue, we extract sample embeddings and obtain explanations from this point onwards, recovering SHAP values by taking the mean over the embedding dimension. The second technique leverages attention activations from the transformer encoder layer to indicate the learned importance of relative token weights within the model. Transformer self-attention layers are multi-headed; in our case, each layer has eight independent heads. We examine all the layers and heads, focusing on the strongest attention weight deviations and investigating their implications.

We showcase the results of the described techniques on a particular sample infected with the "Urelas" trojan<sup>4</sup> which Nebula assigns a maliciousness score of  $f(x) = 0.71$ . We find that integrated gradients and attention activations pinpoint the highest maliciousness indicators within a particular segment shown in [Figure 6](#), which includes a token sequence representing filesystem manipulations. In [Figure 6a](#), integrated gradients suggest that the model leans towards a malicious

<sup>4</sup>SHA1: c7ee95f0ea78400d5e4938e06fea1bb0c388b565



malware analysis applied on assembly instructions. They used a custom architecture called “Galaxy Transformer” to avoid length limitations and construct hierarchical representations. Rudd et al. [47] explored Transformer applicability on static malware detection applied on raw malware bytes. Influenced by the success of the GPT modeling scheme [13], Rudd et al. [47] analyzed Transformer decoder with an autoregressive pre-training objective. Lu et al. [48] use Visual Transformer for pixel-based image analysis that were formed from static properties of malware. Pei et al. [49] apply a hierarchical transformer for code similarity analysis and vulnerability detection. They generate a dataset from benign Linux ELF binaries, obtaining behavioral micro-traces with QEMU based Unicorn emulator.

While some similarities exist between our work and the studies previously mentioned, the application of Transformers in a dynamic malware context, particularly using structured telemetry, distinguishes our approach. Moreover, the comparison with other state-of-the-art dynamic malware detectors and our exploration of the model’s explainability represent additional, distinct contributions with respect to previous work.

## 6 Conclusions, Limitations, and Future Work

In this paper, we present Nebula, a novel self-supervised learning transformer model for dynamic malware detection and classification. We conduct an in-depth ablation study to highlight the effect of each of the components of Nebula on its performance, and how they may influence its decision-making process. This analysis highlights how much the inclusion of different behavioral aspects manifested by malware improves the performance and also how much the data cleaning procedure boosts the accuracy at test time. We compare our approach against previously-proposed machine-learning methods for dynamic malware analysis, in a pure supervised learning setting, and we show that Nebula often achieves better results than CNNs and LSTMs. In particular, Nebula clearly outperforms its competitors on both the Speakeasy and Avast-CTU dataset, when considering the problem of malware classification. To better understand the underlying reasons, we consider two explainability methods, i.e., integrated gradients and attention activations, which use respectively (i) gradient information to compute the attributed importance to each feature, and (ii) the activations of the attention mechanism to highlight which tokens get the maximum focus by the model. Our analysis reveals that Nebula is giving attention to relevant tokens associated with malicious activity by exhibiting long spans of attention.

**Limitations.** To maintain a fair comparison with competing techniques, we did not leverage the self-supervised learning [13, 14] of Nebula, i.e., the possibility of using also unlabeled data to further improve the pretraining step of the transformer architecture. Nevertheless, this is a relevant feature for both malware detection and classification, given the

large availability of unlabeled samples. Another limitation of our work is that, while we have analyzed the predictive performance of Nebula, we have not considered its adversarial robustness against well-crafted, gradient-based attacks aimed to mislead its predictions. While Nebula, as any other approach based on machine learning, may be vulnerable to such powerful attacks, especially in the white-box scenario, it is also worth remarking that, in this case, the attacker may be required to modify the dynamic behavior to obfuscate the malicious activities. In fact, as shown by our explainability analysis, Nebula tends to correctly focus more on portions of reports that contain malicious activities, and hiding them may be more complicated for the attacker than modifying some other spurious features of the input sample. In addition, crafting adversarial malware by manipulating the dynamic behavior without corrupting the original, malicious intent of the source malware remains a complex task. To date, indeed, only some initial attempts have been reported, and no implementation has been released to replicate these attacks [50].

**Future work.** To overcome the aforementioned limitations, we plan to investigate the effect of self-supervised learning on Nebula, pretraining it on a much larger data collection with unlabeled samples. We firmly believe that this approach can further boost its performance, and also enable us to use less supervisions for the downstream tasks. Furthermore, given the tremendous performance of large language models in NLU, we will train Nebula with different report formats together, to study the impact of such heterogeneity on its performances. Finally, we also plan to investigate more in depth the adversarial robustness properties of Nebula, and how to improve them, by developing novel attack algorithms tailored to bypass dynamic malware detectors and classifiers.

## Availability

All the source code used to run the experiments of this work, as well as the pre-trained models, are available to download from GitHub.<sup>5</sup>

## References

- [1] Marcello Cinque, Domenico Cotroneo, and Antonio Pecchia. Challenges and directions in security information and event management (siem). In *2018 IEEE International Symposium on Software Reliability Engineering Workshops (ISSREW)*, pages 95–99, 2018.
- [2] Manya Ali Salitin and Ali Hussein Zolait. The role of user entity behavior analytics to detect network attacks in real time. In *2018 International Conference on Innovation and Intelligence for Informatics, Computing, and Technologies (3ICT)*, pages 1–5, 2018.

<sup>5</sup><https://anonymous.4open.science/r/nebula-3185>

- [3] Dmitrijs Trizna. Quo vadis: Hybrid machine learning meta-model based on contextual and behavioral malware representations. In *Proceedings of the 15th ACM Workshop on Artificial Intelligence and Security, AISEC'22*, page 127–136, New York, NY, USA, 2022. Association for Computing Machinery.
- [4] Chani Jindal, Christopher Salls, Hojjat Aghakhani, Keith Long, Christopher Kruegel, and Giovanni Vigna. Neurlux: Dynamic malware analysis without feature engineering. In *Proceedings of the 35th Annual Computer Security Applications Conference, ACSAC '19*, page 444–455, New York, NY, USA, 2019. Association for Computing Machinery.
- [5] Xiaohui Chen, Zhiyu Hao, Lun Li, Lei Cui, Yiran Zhu, Zhenquan Ding, and Yongji Liu. Cruparamer: Learning on parameter-augmented api sequences for malware detection. *IEEE Transactions on Information Forensics and Security*, 17:788–803, 2022.
- [6] Nilam Nur Amir Sjarif, Suriyati Chuprat, Mohd Naz'ri Mahrin, Noor Azurati Ahmad, Aswami Ariffin, Firham M Senan, Nazri Ahmad Zamani, and Afifah Saupi. Endpoint detection and response: Why use machine learning? In *2019 International Conference on Information and Communication Technology Convergence (ICTC)*, pages 283–288, 2019.
- [7] Wajih Ul Hassan, Adam Bates, and Daniel Marino. Tactical provenance analysis for endpoint detection and response systems. In *2020 IEEE Symposium on Security and Privacy (SP)*, pages 1172–1189, 2020.
- [8] George Karantzas and Constantinos Patsakis. An empirical assessment of endpoint detection and response systems against advanced persistent threats attack vectors. *Journal of Cybersecurity and Privacy*, 1(3):387–421, 2021.
- [9] Zhaoqi Zhang, Panpan Qi, and Wei Wang. Dynamic malware analysis with feature engineering and feature learning. *Proceedings of the AAAI Conference on Artificial Intelligence*, 34:1210–1217, 04 2020.
- [10] Sepp Hochreiter and Jürgen Schmidhuber. Long short-term memory. *Neural Comput.*, 9(8):1735–1780, nov 1997.
- [11] Dzmitry Bahdanau, Kyunghyun Cho, and Yoshua Bengio. Neural machine translation by jointly learning to align and translate. In *International Conference on Learning Representations (ICLR)*, 2015.
- [12] Ashish Vaswani, Noam Shazeer, Niki Parmar, Jakob Uszkoreit, Llion Jones, Aidan N Gomez, Lukas Kaiser, and Illia Polosukhin. Attention is all you need. In I. Guyon, U. Von Luxburg, S. Bengio, H. Wallach, R. Fergus, S. Vishwanathan, and R. Garnett, editors, *Advances in Neural Information Processing Systems*, volume 30, USA, 2017. Curran Associates, Inc.
- [13] Alec Radford and Karthik Narasimhan. Improving language understanding by generative pre-training. *OpenAI*, 2018.
- [14] Jacob Devlin, Ming-Wei Chang, Kenton Lee, and Kristina Toutanova. Bert: Pre-training of deep bidirectional transformers for language understanding, 2019.
- [15] Joshua Saxe and Konstantin Berlin. eXpose: A character-level convolutional neural network with embeddings for detecting malicious urls, file paths and registry keys, 02 2017.
- [16] Adarsh Kyadige, Ethan M. Rudd, and Konstantin Berlin. Learning from context: A multi-view deep learning architecture for malware detection. In *2020 IEEE Security and Privacy Workshops (SPW)*, pages 1–7, USA, 2020. IEEE.
- [17] Karsten Hahn. The real reason why malware detection is hard—and underestimated. *G DATA Security Blog*, June 2022. Online; accessed on June 1, 2023.
- [18] Mukund Sundararajan, Ankur Taly, and Qiqi Yan. Axiomatic attribution for deep networks. In *International conference on machine learning*, pages 3319–3328. PMLR, 2017.
- [19] Jesse Vig. A multiscale visualization of attention in the transformer model. In *Proceedings of the 57th Annual Meeting of the Association for Computational Linguistics: System Demonstrations*, pages 37–42, Florence, Italy, July 2019. Association for Computational Linguistics.
- [20] Branislav Bosansky, Dominik Kouba, Ondrej Manhal, Thorsten Sick, Viliam Lisy, Jakub Kroustek, and Petr Somol. Avast-CTU Public CAPE Dataset, 2022.
- [21] Simon Mandlik, Matej Racinsky, Viliam Lisy, and Tomas Pevny. Mill.jl and jsongrinder.jl: automated differentiable feature extraction for learning from raw json data, 2021.
- [22] Xiaohui Chen, Ying Tong, Chunlai Du, Yongji Liu, Zhenquan Ding, Qingyun Ran, Yi Zhang, Lei Cui, and Zhiyu Hao. Malpro: Learning on process-aware behaviors for malware detection. In *2022 IEEE Symposium on Computers and Communications (ISCC)*, pages 01–07, 2022.
- [23] Verizon Communications. Verizon Data Breach Investigation Report (DBIR). <https://www.verizon.com/>

- [business/resources/reports/dbir/2022/results-and-analysis-intro/](https://business/resources/reports/dbir/2022/results-and-analysis-intro/), 2022. Online; accessed on May 31, 2023.
- [24] Alessandro Mantovani, Simone Aonzo, Yanick Fratantonio, and Davide Balzarotti. RE-Mind: a first look inside the mind of a reverse engineer. In *31st USENIX Security Symposium (USENIX Security 22)*, pages 2727–2745, Boston, MA, August 2022. USENIX Association.
- [25] Kilian Weinberger, Anirban Dasgupta, John Langford, Alex Smola, and Josh Attenberg. Feature hashing for large scale multitask learning. In *Association for Computing Machinery, ICML '09*, page 1113–1120, New York, NY, USA, 2009. Association for Computing Machinery.
- [26] Steven Bird, Ewan Klein, and Edward Loper. *Natural language processing with Python: analyzing text with the natural language toolkit*. " O'Reilly Media, Inc.", 2009.
- [27] Danny Hendler, Shay Kels, and Amir Rubin. Amsi-based detection of malicious powershell code using contextual embeddings. In *Proceedings of the 15th ACM Asia Conference on Computer and Communications Security*, pages 679–693, 2020.
- [28] Dmitrijs Trizna. Shell Language Processing: Unix command parsing for machine learning. *Proceedings of Conference on Applied Machine Learning for Information Security (CAMLIS)*, 2021, 2021.
- [29] Rico Sennrich, Barry Haddow, and Alexandra Birch. Neural machine translation of rare words with subword units. In *Proceedings of the 54th Annual Meeting of the Association for Computational Linguistics (Volume 1: Long Papers)*, pages 1715–1725, Berlin, Germany, August 2016. Association for Computational Linguistics.
- [30] Taku Kudo and John Richardson. SentencePiece: A simple and language independent subword tokenizer and detokenizer for neural text processing. In *Proceedings of the 2018 Conference on Empirical Methods in Natural Language Processing: System Demonstrations*, pages 66–71, Brussels, Belgium, November 2018. Association for Computational Linguistics.
- [31] Claude Sammut and Geoffrey I. Webb, editors. *TF-IDF*, pages 986–987. Springer US, Boston, MA, 2010.
- [32] Jose Camacho-Collados and Mohammad Taher Pilehvar. Embeddings in natural language processing. In *Proceedings of the 28th International Conference on Computational Linguistics: Tutorial Abstracts*, pages 10–15, Barcelona, Spain (Online), December 2020. International Committee for Computational Linguistics.
- [33] Mandiant. Speakeasy: portable, modular, binary emulator designed to emulate Windows kernel and user mode malware., 11 2021. <https://github.com/mandiant/speakeasy>.
- [34] Sébastien Bubeck, Varun Chandrasekaran, Ronen Eldan, Johannes Gehrke, Eric Horvitz, Ece Kamar, Peter Lee, Yin Tat Lee, Yuanzhi Li, Scott Lundberg, Harsha Nori, Hamid Palangi, Marco Tulio Ribeiro, and Yi Zhang. Sparks of artificial general intelligence: Early experiments with gpt-4, 2023.
- [35] Simone Aonzo, Yufei Han, Alessandro Mantovani, and Davide Balzarotti. Humans vs. machines in malware classification. In *32nd USENIX Security Symposium (USENIX Security 23)*, Anaheim, CA, August 2023. USENIX Association.
- [36] Jonas Gehring, Michael Auli, David Grangier, Denis Yarats, and Yann N. Dauphin. Convolutional sequence to sequence learning. In Doina Precup and Yee Whye Teh, editors, *Proceedings of the 34th International Conference on Machine Learning*, volume 70 of *Proceedings of Machine Learning Research*, pages 1243–1252. PMLR, 06–11 Aug 2017.
- [37] Jared Kaplan, Sam McCandlish, Tom Henighan, Tom B. Brown, Benjamin Chess, Rewon Child, Scott Gray, Alec Radford, Jeffrey Wu, and Dario Amodei. Scaling laws for neural language models, 2020.
- [38] A. Brukhovetsky and K. O'Reilly. Cape sandbox v2.1 book, 2022. Accessed on 08/01/2022.
- [39] Cuckoo Foundation. Cuckoo sandbox. <https://github.com/cuckoosandbox/cuckoo>. Online; accessed on May 30, 2023.
- [40] Malicious Code Data Set, Jul 2019. <https://github.com/kericwyl337/Datacon2019-Malicious-Code-DataSet-Stage1>.
- [41] Ilya Loshchilov and Frank Hutter. Decoupled weight decay regularization, 2019.
- [42] Cybersecurity and Infrastructure Security Agency. Emotet Malware. <https://www.cisa.gov/news-events/alerts/2018/07/20/emotet-malware>, January 2020. Online; accessed on June 1, 2023.
- [43] Brian Krebs. 'Operation Tovar' Targets 'GameOver' ZeuS Botnet, CryptoLocker Scourge. *KrebsOnSecurity*, June 2014. Online; accessed on June 1, 2023.
- [44] Scott M Lundberg and Su-In Lee. A unified approach to interpreting model predictions. In I. Guyon, U. V. Luxburg, S. Bengio, H. Wallach, R. Fergus, S. Vishwanathan, and R. Garnett, editors, *Advances in Neural*

*Information Processing Systems 30*, pages 4765–4774. Curran Associates, Inc., 2017.

- [45] Check Point Research. Anti-Debug: Timing. <https://anti-debug.checkpoint.com/techniques/timing.html>. Online; accessed on June 5, 2023.
- [46] Miles Q. Li, Benjamin C.M. Fung, Philippe Charland, and Steven H.H. Ding. I-MAD: Interpretable malware detector using galaxy transformer. *Computers and Security*, 108:102371, sep 2021.
- [47] Ethan M. Rudd, Mohammad Saidur Rahman, and Philip Tully. Transformers for end-to-end infosec tasks: A feasibility study. In *Proceedings of the 1st Workshop on Robust Malware Analysis, WoRMA '22*, page 21–31, New York, NY, USA, 2022. Association for Computing Machinery.
- [48] Qikai Lu, Hongwen Zhang, Husam Kinawi, and Di Niu. Self-attentive models for real-time malware classification. *IEEE Access*, 10:95970–95985, 2022.
- [49] Kexin Pei, Zhou Xuan, Junfeng Yang, Suman Jana, and Baishakhi Ray. Learning approximate execution semantics from traces for binary function similarity. *IEEE Transactions on Software Engineering*, 49(4):2776–2790, 2023.
- [50] Ishai Rosenberg, Asaf Shabtai, Lior Rokach, and Yuval Elovici. Generic black-box end-to-end attack against state of the art api call based malware classifiers. In *Research in Attacks, Intrusions, and Defenses: 21st International Symposium, RAID 2018, Heraklion, Crete, Greece, September 10-12, 2018, Proceedings 21*, pages 490–510. Springer, 2018.

## A Malware Classification Result Tables

Below we present detailed malware classification results with evaluation metrics per each malware type on Speakeasy Dataset [3] in Table 11 and per each malware family on Avast-CTU Dataset [20] in Table 12.

Table 11: Malware classification results on Speakeasy Dataset. Reported TPR is at FPR=  $10^{-3}$ .

(a) Validation set					(b) Test Set				
Model	TPR	AUC	F1	Accuracy	TPR	AUC	F1	Accuracy	
Benignware					Benignware				
Gated CNN [9]	0.114	0.9209	0.8793	0.9166	Gated CNN [9]	0.0229	0.7482	0.7588	0.736
Neurlux [4]	0.3486	<b>0.9756</b>	0.9609	0.9741	Neurlux [4]	0.0347	0.8464	0.8453	0.8362
Quo.Vadis [3]	<b>0.4605</b>	0.958	0.9463	0.9655	Quo.Vadis [3]	<b>0.0395</b>	0.8385	0.8337	0.8327
Nebula (BPE)	0.4475	0.9729	<b>0.9613</b>	<b>0.9748</b>	Nebula (BPE)	0.0382	<b>0.8555</b>	<b>0.8526</b>	<b>0.8468</b>
Backdoor					Backdoor				
Gated CNN [9]	0.6974	0.8456	0.8059	0.952	Gated CNN [9]	0.4102	0.7894	0.687	0.9395
Neurlux [4]	0.6586	<b>0.9223</b>	0.8929	0.9704	Neurlux [4]	0.7382	0.8663	0.8329	0.9671
Quo.Vadis [3]	<b>0.7898</b>	0.8924	0.8711	0.9661	Quo.Vadis [3]	0.7741	0.8839	0.852	0.97
Nebula (BPE)	0.775	0.9209	<b>0.8965</b>	<b>0.9716</b>	Nebula (BPE)	<b>0.7851</b>	<b>0.889</b>	<b>0.8548</b>	<b>0.9703</b>
Coinminer					Coinminer				
Gated CNN [9]	0.553	0.8917	0.801	0.9634	Gated CNN [9]	0.1066	0.7853	0.5586	0.9004
Neurlux [4]	<b>0.8938</b>	<b>0.9445</b>	<b>0.923</b>	<b>0.9865</b>	Neurlux [4]	<b>0.4913</b>	<b>0.7858</b>	<b>0.691</b>	<b>0.9495</b>
Quo.Vadis [3]	0.8477	0.9288	0.8811	0.9788	Quo.Vadis [3]	0.083	0.724	0.4884	0.8964
Nebula (BPE)	0.8804	0.9371	0.9083	0.9839	Nebula (BPE)	0.2468	0.7705	0.6303	0.9355
Dropper					Dropper				
Gated CNN [9]	0.2407	0.8793	0.7665	0.9477	Gated CNN [9]	0.1063	0.6901	0.2015	0.9517
Neurlux [4]	<b>0.4505</b>	<b>0.9659</b>	<b>0.8895</b>	<b>0.9741</b>	Neurlux [4]	<b>0.4433</b>	<b>0.8294</b>	<b>0.4488</b>	0.9669
Quo.Vadis [3]	0.3434	0.959	0.8704	0.9695	Quo.Vadis [3]	0.2299	0.7948	0.358	0.968
Nebula (BPE)	0.4148	0.9482	0.8742	0.9714	Nebula (BPE)	0.1846	0.7097	0.285	<b>0.9673</b>
Keylogger					Keylogger				
Gated CNN [9]	0.4601	0.8403	0.7177	0.9689	Gated CNN [9]	<b>0.0527</b>	0.5215	0.0794	<b>0.9418</b>
Neurlux [4]	<b>0.6925</b>	0.9503	<b>0.8576</b>	<b>0.9826</b>	Neurlux [4]	0.0519	0.5699	0.2032	0.9189
Quo.Vadis [3]	0.3644	<b>0.9577</b>	0.7961	0.9723	Quo.Vadis [3]	0.0388	<b>0.5848</b>	<b>0.2119</b>	0.8981
Nebula (BPE)	0.5685	0.9376	0.8293	0.9789	Nebula (BPE)	0.0306	0.5362	0.1295	0.9124
Ransomware					Ransomware				
Gated CNN [9]	0.9252	0.9587	0.9356	0.9839	Gated CNN [9]	0.2318	0.6112	0.3584	0.899
Neurlux [4]	0.961	0.9793	0.9732	0.9933	Neurlux [4]	0.3969	0.6949	0.5527	0.923
Quo.Vadis [3]	<b>0.9839</b>	<b>0.9908</b>	<b>0.9844</b>	<b>0.9961</b>	Quo.Vadis [3]	0.5385	0.7659	0.6861	0.9398
Nebula (BPE)	0.9713	0.9833	0.9699	0.9924	Nebula (BPE)	<b>0.6154</b>	<b>0.804</b>	<b>0.7421</b>	<b>0.9476</b>
RAT					RAT				
Gated CNN [9]	0.0381	0.5142	0.052	0.9782	Gated CNN [9]	0.0099	0.4999	0.0	0.9276
Neurlux [4]	<b>0.5047</b>	<b>0.7497</b>	<b>0.6564</b>	<b>0.9884</b>	Neurlux [4]	<b>0.5044</b>	<b>0.7495</b>	<b>0.6625</b>	<b>0.9632</b>
Quo.Vadis [3]	0.2861	0.6387	0.3688	0.9806	Quo.Vadis [3]	0.0598	0.5326	0.1195	0.9245
Nebula (BPE)	0.4171	0.7053	0.5618	0.9857	Nebula (BPE)	0.2425	0.6171	0.3683	0.9426
Trojan					Trojan				
Gated CNN [9]	0.1253	0.8425	0.6891	0.9156	Gated CNN [9]	0.1483	0.7705	0.5282	0.9355
Neurlux [4]	<b>0.3903</b>	0.8827	<b>0.8022</b>	<b>0.9516</b>	Neurlux [4]	<b>0.3087</b>	0.8254	0.6153	0.9426
Quo.Vadis [3]	0.2007	0.8788	0.7666	0.9391	Quo.Vadis [3]	0.1656	0.7674	0.5359	0.9386
Nebula (BPE)	0.2268	<b>0.8878</b>	0.7853	0.9442	Nebula (BPE)	0.2413	<b>0.8688</b>	<b>0.6827</b>	<b>0.9551</b>

Table 12: Results of Multi-label classification over 10 labels on Avast-CTU dataset [20]. Reported TPR is at FPR=  $10^{-3}$ .

(a) Validation set					(b) Test set				
Model	TPR	AUC	F1	Accuracy	Model	TPR	AUC	F1	Accuracy
Adload					Adload				
Neurlux [4]	<b>0.9927</b>	<b>0.9963</b>	<b>0.995</b>	<b>0.9998</b>	Neurlux [4]	0.7314	<b>0.9991</b>	<b>0.715</b>	0.9983
Nebula (BPE)	0.9686	0.984	0.9685	0.9988	Nebula (BPE)	0.5447	0.866	0.439	0.9985
Nebula (whitesp.)	0.9768	0.9881	0.9738	0.999	Nebula (whitesp.)	<b>0.8248</b>	0.9664	0.6975	<b>0.9994</b>
Emotet					Emotet				
Neurlux [4]	<b>0.7329</b>	<b>0.9968</b>	<b>0.9957</b>	<b>0.9975</b>	Neurlux [4]	<b>0.7244</b>	0.9345	0.9294	0.9593
Nebula (BPE)	0.4572	0.9962	0.9936	0.9962	Nebula (BPE)	0.1806	<b>0.9453</b>	<b>0.9392</b>	<b>0.9643</b>
Nebula (whitesp.)	0.2601	0.9958	0.9929	0.9959	Nebula (whitesp.)	0.4537	0.9381	0.9319	0.9604
Harhar					Harhar				
Neurlux [4]	<b>1.0</b>	<b>1.0</b>	<b>0.9975</b>	<b>0.9999</b>	Neurlux [4]	<b>0.8697</b>	<b>0.9347</b>	<b>0.9031</b>	<b>0.999</b>
Nebula (BPE)	0.9965	0.9982	0.995	0.9998	Nebula (BPE)	0.667	0.8333	0.7763	0.998
Nebula (whitesp.)	0.9965	0.9982	0.9958	0.9999	Nebula (whitesp.)	0.7394	0.8696	0.8363	0.9984
Lokibot					Lokibot				
Neurlux [4]	<b>0.529</b>	<b>0.981</b>	<b>0.9727</b>	<b>0.9949</b>	Neurlux [4]	0.0697	0.943	0.832	0.9777
Nebula (BPE)	0.3231	0.9729	0.9565	0.9919	Nebula (BPE)	0.1583	0.9499	0.8957	0.9872
Nebula (whitesp.)	0.2655	0.9781	0.9595	0.9924	Nebula (whitesp.)	<b>0.2802</b>	<b>0.9561</b>	<b>0.9048</b>	<b>0.9882</b>
Qakbot					Qakbot				
Neurlux [4]	<b>0.9946</b>	<b>0.9971</b>	<b>0.9956</b>	<b>0.999</b>	Neurlux [4]	0.4172	0.9945	0.932	0.9949
Nebula (BPE)	0.9869	0.9932	0.992	0.9981	Nebula (BPE)	<b>0.9839</b>	0.9918	<b>0.9876</b>	<b>0.9992</b>
Nebula (whitesp.)	0.8387	0.9934	0.9906	0.9977	Nebula (whitesp.)	0.7505	<b>0.9955</b>	0.9768	0.9984
Swisyn					Swisyn				
Neurlux [4]	<b>0.999</b>	<b>0.9994</b>	<b>0.9993</b>	<b>0.9997</b>	Neurlux [4]	<b>0.9987</b>	<b>0.9992</b>	<b>0.9991</b>	<b>0.9993</b>
Nebula (BPE)	0.9972	0.9985	0.9983	0.9993	Nebula (BPE)	0.7396	0.9978	0.9973	0.998
Nebula (whitesp.)	0.9978	0.9989	0.9988	0.9995	Nebula (whitesp.)	0.9972	0.9985	0.9984	0.9988
Trickbot					Trickbot				
Neurlux [4]	0.6086	<b>0.9954</b>	<b>0.986</b>	<b>0.9978</b>	Neurlux [4]	<b>0.1137</b>	<b>0.9811</b>	<b>0.9536</b>	<b>0.989</b>
Nebula (BPE)	<b>0.662</b>	0.9913	0.9825	0.9973	Nebula (BPE)	0.0573	0.9749	0.9227	0.9811
Nebula (whitesp.)	0.5446	0.9928	0.9813	0.9971	Nebula (whitesp.)	0.0389	<b>0.9811</b>	0.9056	0.976
Ursnif					Ursnif				
Neurlux [4]	<b>0.9524</b>	<b>0.9761</b>	<b>0.9698</b>	<b>0.9987</b>	Neurlux [4]	<b>0.8287</b>	0.914	0.891	0.9918
Nebula (BPE)	0.7346	0.9435	0.918	0.9964	Nebula (BPE)	0.7307	0.9532	0.9362	0.9947
Nebula (whitesp.)	0.857	0.9562	0.9407	0.9974	Nebula (whitesp.)	0.7875	<b>0.9684</b>	<b>0.9585</b>	<b>0.9965</b>
Zeus					Zeus				
Neurlux [4]	<b>0.4228</b>	<b>0.9817</b>	<b>0.9663</b>	<b>0.9956</b>	Neurlux [4]	0.0811	<b>0.9537</b>	0.6503	0.9875
Nebula (BPE)	0.3593	0.9638	0.9411	0.9923	Nebula (BPE)	<b>0.1007</b>	0.917	0.6419	0.9873
Nebula (whitesp.)	0.4016	0.9663	0.9474	0.9932	Nebula (whitesp.)	0.1	0.9192	<b>0.669</b>	<b>0.9894</b>
Njrat					Njrat				
Neurlux [4]	<b>0.233</b>	<b>0.9858</b>	<b>0.9606</b>	<b>0.994</b>	Neurlux [4]	0.0633	<b>0.9827</b>	0.8479	0.9831
Nebula (BPE)	0.1347	0.975	0.9329	0.9896	Nebula (BPE)	0.078	0.9745	0.8656	0.9858
Nebula (whitesp.)	0.2328	0.9727	0.945	0.9916	Nebula (whitesp.)	<b>0.1263</b>	0.9716	<b>0.8896</b>	<b>0.9887</b>